
🌀 VIT-LENS: Initiating Omni-Modal Exploration through 3D Insights

Weixian Lei^{1,2,3} Yixiao Ge^{2†} Jianfeng Zhang³ Dylan Sun² Kun Yi²
Ying Shan² Mike Zheng Shou^{1,3†}

¹Show Lab,³National University of Singapore ²ARC Lab, Tencent PCG

<https://github.com/TencentARC/ViT-Lens>

Abstract

Though the success of CLIP-based training recipes in vision-language models, their scalability to more modalities (e.g., 3D, audio, etc.) is limited to large-scale data, which is expensive or even inapplicable for rare modalities. In this paper, we present VIT-LENS that facilitates efficient omni-modal representation learning by perceiving novel modalities with a pretrained-ViT and aligning to a pre-defined space. Specifically, the modality-specific lens is tuned to project multimodal signals to the shared embedding space, which are then processed by a strong ViT that carries pre-trained image knowledge. The encoded multimodal representations are optimized toward aligning with the modal-independent space, pre-defined by off-the-shelf foundation models. A well-trained lens with a ViT backbone has the potential to serve as one of these foundation models, supervising the learning of subsequent modalities. VIT-LENS provides a unified solution for representation learning of increasing modalities with two appealing benefits: (i) Exploiting the pretrained-ViT across tasks and domains effectively with efficient data regime; (ii) Emergent downstream capabilities of novel modalities are demonstrated due to the modality alignment space. We evaluate VIT-LENS in the context of 3D as an initial verification. In zero-shot 3D classification, VIT-LENS achieves substantial improvements over previous state-of-the-art, showing **52.0%** accuracy on Objaverse-LVIS, **87.4%** on ModelNet40, and **60.6%** on ScanObjectNN. Furthermore, we enable zero-shot 3D question-answering by simply integrating the trained 3D lens into the InstructBLIP model without any adaptation. We will release the results of VIT-LENS on more modalities in the near future.

1 Introduction

Omni-modal representation learning has emerged as a focal point of research, garnering a surge of interest owing to its relevance in real-world applications like Embodied AI. In the uni-modal realm, the community has harnessed the versatility of Transformers [62] in conjunction with the abundance of large-scale web data, yielding notable successes in the development of general-purpose foundation models for Natural Language Processing [12, 41, 57, 58, 5, 49] and Computer Vision [13, 28, 4, 53, 17, 16]. In cross-modal research, the vision-language model CLIP [56] stands as a significant milestone by capitalizing on large-scale image-text paired data for pertaining. While proficient in integrating vision and language, the present CLIP-based models are constrained in their ability to encompass and interpret additional sensory modalities, such as audio, depth, and 3D shape.

[†]Corresponding authors.

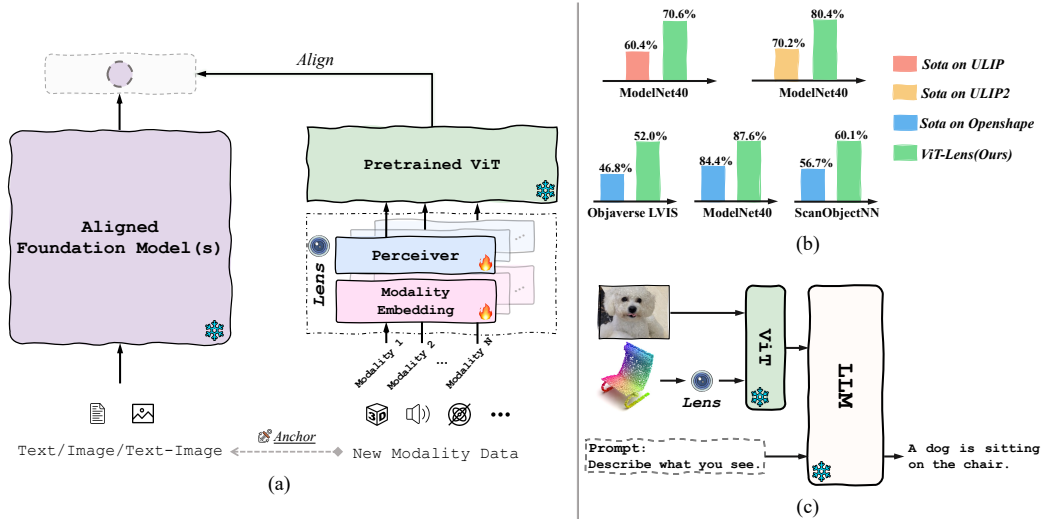


Figure 1: **(a) Illustration of VIT-LENS.** VIT-LENS extends the capabilities of a pretrained-ViT to perceive and comprehend diverse modalities beyond 2D images. It achieves this by firstly employing Modality Embedding and the Perceiver architecture [29] to map modality-specific data into the pretrained-ViT input space. Then the encoded output of ViT is aligned with the feature extracted from the data’s anchor text/image/text-image, through an off-the-shelf foundation model. This novel approach enables a pretrained-ViT to integrate and understand diverse modalities beyond images while leveraging its knowledge from the pretraining to better comprehend and interpret these modalities. **(b) Zero-shot 3D classification.** Our VIT-LENS outperforms the state-of-the-art methods on zero-shot 3D classification when pretrained on datasets introduced by ULIP [68], ULIP2 [69] and OpenShape [40] respectively. **(c) Emergent Downstream Abilities.** By incorporating new modalities into the ViT of an off-the-shelf MLLM, VIT-LENS empowers the LLM to understand novel modalities or their combinations, without any tailored instruction-following tuning.

Several recent works, *e.g.*, ImageBind [22] and ONE-PEACE [63], have initiated the pursuit of constructing a representation model that can encompass a wide range of modalities. With either modality-specific encoders or a modality-shared architecture, they heavily rely on large-scale data with cross-modal aligned semantics (*e.g.*, paired with image or text), which inevitably hinders their ability for accommodating an extensive variety of modalities. Specifically, gathering large-scale data for certain modalities can be non-trivial. This leads to sub-optimal models with poor generalization when facing novel categories, thus hindering their wider applications in the real world.

In this work, we present a novel perspective. Given the exceptional generalization and transfer learning capabilities of the pretrained-ViT models [56, 17, 16, 6, 51], there is promise in adapting the inherent knowledge to comprehend novel modalities, without the need for collecting large-scale data to train models from scratch for each modality, which demands substantial time and resources. Recognizing the rich knowledge encoded in a pretrained-ViT, we conjecture that a pretrained-ViT is able to function as a multi-modal processor – it possesses the capacity to sense and comprehend a spectrum of modalities as it interprets images.

From this standpoint, we introduce VIT-LENS, which encodes the out-of-image modalities through a pretrained-ViT, with the goal of maximizing the utilization of pretrained model weights and the knowledge they encapsulate. As illustrated in Figure 1, VIT-LENS integrates a modality embedding module and a perceiver [29] to map input data into the pretrained-ViT input space. Subsequently, a frozen pretrained-ViT is applied for further encoding. This approach enables the encoding of diverse modalities, aligning their features with the established features of anchor data, be it images, text, or image-text, through an off-the-shelf foundation model.

Our proposed method offers several advantages in advancing omni-modal representation learning: (1) **Model Unification.** Our VIT-LENS adopts a shared pretrained-ViT for various modalities, facilitating scalable modality extension and aligning with the growing trend of big convergence in multi-modal

understanding [64]. (2) **Data-Efficient Approach.** VIT-LENS achieves its versatility and applicability across diverse tasks and domains by effectively utilizing the advanced ViT model without the need for large-scale data. (3) **Emergent Ability.** Recent studies in Multimodal Large Language Models (MLLMs) [34, 1, 50, 78, 39, 10] have underscored the essential role of vision representation models to unleash Large Language Models (LLMs) to perceive and understand the visual world. Interestingly, we find that by binding a new modality to the ViT used in an off-the-shelf MLLM, the corresponding LLM can seamlessly sense and comprehend that modality without any specific instruction tuning.

To demonstrate the effectiveness of VIT-LENS, we evaluate its performance in the context of 3D shape understanding. Specifically, we follow the pre-training paradigms of prior works [68, 69, 40], but aims to establish a more generalized and scalable joint representation space encompassing 2D images, text and 3D shapes by binding 3D point cloud to a pretrained-ViT. On the zero-shot 3D shape classification task, VIT-LENS exhibits substantial improvements over previous zero-shot state-of-the-art methods. Notably, using the same datasets for pretraining, VIT-LENS outperforms ULIP [68] by **10.2%**, ULIP2 [69] by **10.4%**, and OpenShape [40] by **3.2%** on ModelNet40 [66] in terms of zero-shot accuracy. VIT-LENS also excels at handling long-tail categories. On the challenging Objaverse-LVIS dataset [11] containing 1,156 categories, VIT-LENS achieves a **52.0%** zero-shot accuracy, significantly surpassing previous SOTA by **5.2%**.

Besides zero-shot classification, we bind 3D shapes to the ViT architecture employed in InstructBlip [10], an MLLM capable of understanding and interacting over 2D images. After pretraining, we plug the 3D encoder produced by VIT-LENS into InstructBlip to investigate whether VIT-LENS can bestow the LLM with the ability to perceive and comprehend the 3D modality. This integration showcases that the new variant of the MLLM is endowed with the capability for 3D shape captioning and question answering, without necessitating specific instruction tuning.

VIT-LENS aims to pursue omni-modal representation learning in a simple yet effective manner, alleviating the need for large-scale data collection and utilizing a single set of knowledge expert parameters. Our initial exploration strives to enable Large Language Models (LLMs) to sense and comprehend out-of-image modalities in a zero-shot manner. Future work can further scale up training to extend VIT-LENS to more modalities and explore additional emergent abilities.

2 VIT-LENS for 3D Shape Understanding

VIT-LENS assimilates the pre-training framework in [68, 69, 40] and introduces to learn 3D shape representation through a pretrained-ViT. In this context, we use CLIP-ViT, which allows VIT-LENS to leverage the rich knowledge from the large-scale image-text data, adopting the transferability of the original CLIP-ViT model. By extending this paradigm to encompass more modalities, VIT-LENS not only enables a ViT to seamlessly sense and comprehend 3D shapes but also allows it to understand other modalities as it digests images, all while utilizing a single set of model parameters.

2.1 Preliminary: CLIP for 3D Shape Representation Learning

CLIP (Contrastive Language-Image Pretraining) is a powerful multimodal model trained on a large dataset of image-text pairs. It learns to map images and their corresponding text into a shared embedding space through contrastive learning. The resulting joint image-text embeddings enable CLIP to perform various multimodal tasks, showcasing remarkable generalization and zero-shot learning capabilities. CLIP’s knowledge, acquired from extensive pretraining on image-text data, encapsulates rich information about the visual world and language. This inherent knowledge makes CLIP highly transferable, allowing it to excel in downstream tasks and domains without task-specific fine-tuning.

Building upon CLIP, ULIP [68] introduces an efficient multimodal pretraining framework using triplets that encompass three modalities: (1) the 3D modality, extracted from 3D point cloud data; (2) the image modality, generated by rendering images from 3D object files with multiple viewpoints; and (3) the language modality, derived by converting dataset metadata into coherent sentences, including descriptive terms and category names. Subsequently, [69, 40] scale up the pretraining 3D data and leverage a large language model [35, 34, 50] to automatically generate detailed captions from a comprehensive set of holistic views, reducing reliance on human annotations. All these methods learn 3D shape representations aligned with the pretrained CLIP embedding spaces of language and

image. VIT-LENS follows the same training paradigm as these works but incorporates the pretrained vision part for 3D shape encoding, aiming to utilize the CLIP-ViT from the model perspective.

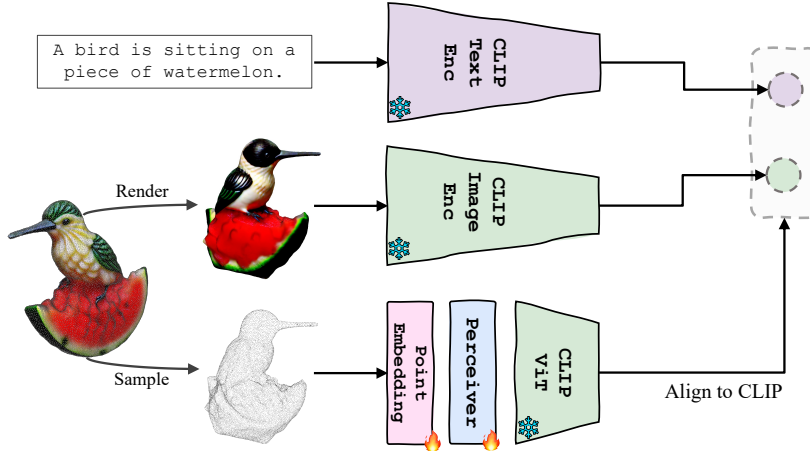


Figure 2: **Training pipeline of VIT-LENS for 3D shape understanding.** VIT-LENS aligns the triplet of 3D point clouds, 2D rendered images, and textual descriptions to a unified feature space, defined by CLIP. It leverages the capabilities of a powerful pretrained vision language model, CLIP [56, 8], which is frozen during pretraining and provides a pre-aligned feature space. The 3D shape encoder consists of a point embedding layer, a Perceiver, and a pretrained CLIP-ViT, shared with the image encoder. To enhance 3D point cloud encoding, point embeddings are obtained and distilled through the Perceiver before feeding into the frozen CLIP-ViT to obtain the final representation. The training objective is to minimize the contrastive loss for aligning features in the shared feature space.

2.2 Architecture

Text and Image Encoders. VIT-LENS aligns the triplet of 3D point clouds, 2D rendered images, and comprehensive descriptions to a unified feature space. As depicted in Figure 2, we leverage the capabilities of a powerful pretrained vision language model, CLIP [56, 8], and freeze it during pretraining. The feature space, which has already been pre-aligned by CLIP, serves as the target space where we aim to integrate the 3D modality.

3D Shape Encoder. As is shown in Figure 2, the model architecture of 3D encoder in VIT-LENS consists of a point embedding layer [72], a Perceiver [29] and a pretrained CLIP-ViT. Due to the distinct characteristics of different modalities, directly inputting the 3D point cloud into the pretrained CLIP-ViT can lead to a mismatch in the input space, resulting in suboptimal performance even with the use of a powerful model. Therefore, we employ some heuristic designs prior to CLIP-ViT for better 3d point cloud encoding: (1) *Obtain point embeddings*: we first partition the input point clouds into several point patches (sub-clouds) and then map them into a sequence of point embeddings [72]; (2) *Map point embeddings into CLIP-ViT input space*: we apply the Perceiver architecture [29] to iteratively distill the point embeddings into a group of latent embeddings, thereby constructing the input for CLIP-ViT. Subsequently, the latent embeddings are forwarded to the frozen CLIP-ViT to obtain the final 3D representation.

During pretraining, CLIP-ViT remains frozen, and only the parameters of point embedding and Perceiver are updated. This design philosophy is equally applicable across other modalities. This modulated architecture not only retains the foundational knowledge ingrained within the ViT model, but also realizes computational efficiency in comparison to training the entire encoder.

Perceiver: Connecting Modalities to CLIP-ViT. Notably, the Perceiver architecture leverages an asymmetric attention mechanism to iteratively distill inputs into a tight latent bottleneck, allowing it to handle very large inputs of arbitrary sizes and thus can accommodate different modalities. Similar architectures are employed in Vision-Language Models (VLMs) like Flamingo [1] and BLIP-2 [34] to extract visual information for Large Language Models (LLMs). However, VIT-LENS takes a novel approach by using the Perceiver to map input signals from various modalities into the input

space of the pretrained CLIP-ViT, unleashing CLIP-ViT to sense and comprehend other modalities beyond images. This innovative design enables VIT-LENS to achieve omni-modal representations in a straightforward and efficient manner.

Multimodal Representation Alignment. We train the 3D encoder that takes 3D point clouds as input and extracts 3D shape feature. Following the approach in previous works [68, 69, 40], we adopt multimodal contrastive learning for representation alignment. Given the 3D encoder F^P , the frozen CLIP image encoder F^I , and the frozen CLIP text encoder F^T , along with a sampled batch of triplets $\{(P_i, I_i, T_i)\}$ for the 3D point clouds of a shape, its corresponding rendered image, and the associated text, the contrastive loss for alignment is formulated as:

$$\mathcal{L} = -\frac{1}{4B} \sum_{i=1}^B \left(\underbrace{\log \frac{\exp(h_i^P \cdot h_i^I / \tau)}{\sum_j \exp(h_i^P \cdot h_j^I / \tau)} + \log \frac{\exp(h_i^I \cdot h_i^P / \tau)}{\sum_j \exp(h_i^I \cdot h_j^P / \tau)}}_{\mathcal{L}_{P2I}: \text{Point Cloud-Image contrastive}} + \underbrace{\log \frac{\exp(h_i^P \cdot h_i^T / \tau)}{\sum_j \exp(h_i^P \cdot h_j^T / \tau)} + \log \frac{\exp(h_i^T \cdot h_i^P / \tau)}{\sum_j \exp(h_i^T \cdot h_j^P / \tau)}}_{\mathcal{L}_{P2T}: \text{Point Cloud-Text contrastive}} \right),$$

where B is the number of shapes in a batch; τ is a learnable temperature; $h_i^P = F^P(P_i) / \|F^P(P_i)\|$, $h_i^I = F^I(I_i) / \|F^I(I_i)\|$ and $h_i^T = F^T(T_i) / \|F^T(T_i)\|$ denote normalized features of P_i , I_i and T_i . The objective of training the 3D encoder is to minimize \mathcal{L} .

3 Experiments

3.1 Experimental Setting

Pretraining Datasets. Our experimental setup for pretraining leverages datasets from prior works [68, 69, 40] at varying scales: **►ULIP-ShapeNet Triplets** [68] are derived from ShapeNet55 [7], where point clouds are generated from CAD models. Images are synthesized using virtual cameras positioned around each object, and texts are obtained by filling metadata into a predefined prompt template. **►ULIP2-Objaverse Triplets** [69] utilize the recently released Objaverse [11]. For each 3D object, 12 rendered images are used, spaced equally by 360/12 degrees. Each rendered image has 10 detailed captions generated using BLIP2-opt6.7B [34]. **►OpenShape Triplets** [40] encompass four prominent public 3D datasets: ShapeNet [7], 3D-FUTURE [19], ABO [9], and Objaverse [11]. For each 3D object, 12 color images are rendered from preset camera poses, and thumbnail images are included as candidates if provided. OpenShape employs various strategies to obtain high-quality text descriptions, including filtering noisy metadata using GPT4 [50], generating captions using BLIP [35] and Azure cognition services, and conducting image retrieval on LAION-5B to retrieve relevant texts with paired images closely resembling the object’s rendered image, leading to a wider range of text styles. We show the statistics of the pretraining datasets in Table.1.

Table 1: Statistics of pretraining datasets.

Dataset	Source	# 3D point clouds
►ULIP-ShapeNet Triplets	ShapeNet [7]	~52.5k
►ULIP2-Objaverse Triplets	Objaverse [11]	~798.8k
►OpenShape Triplets	ShapeNet [7], 3D-FUTURE [19], ABO [9], Objaverse [11]	~876k

Table 2: CLIP models used in experiments.

CLIP Model	Source	CLIP PT Dataset
OpenAI-B16	OpenAI	WIT-400M
Laion2B-B16	OpenCLIP	LAION-2B
OpenAI-L14	OpenAI	WIT-400M
Datacomp-L14	OpenCLIP	DataComp-1B
EVA01-g14	BAAI	LAION-400M
bigG14	OpenCLIP	LAION-2B

Downstream Datasets. We use the following datasets for downstream tasks. (i) ModelNet40 [66] is a synthetic dataset of 3D CAD models with 9,843 training samples and 2,468 testing samples, covering 40 categories. (ii) ScanObjectNN [61] is a dataset of scanned 3D objects from the real world, containing 2,902 objects categorized into 15 categories. We follow [68, 69, 40] and use the variants

provided by [72] in our experiments. (iii) Objaverse-LVIS is an annotated subset of Objaverse [11], comprising 46,832 shapes from 1,156 LVIS [26] categories. With a larger base of classes compared to other benchmarks, Objaverse-LVIS presents a challenging long-tailed distribution, making it a better reflection of the model’s performance in open-world scenarios.

Implementation Details. In our 3D shape understanding experiments, we employ CLIP models [56, 8] to encode text descriptions and rendered images. The specific CLIP models used in our experiments are outlined in Table 2. The CLIP-ViT version, serving as the CLIP image encoder, is directly integrated into the 3D encoder *by default*.

Regarding data preprocessing, we uniformly sample 8,192 points for ▶ULIP-ShapeNet Triplets, ▶ULIP2-Objaverse Triplets, and 10,000 points for ▶OpenShape-Triplets. These 3D inputs are further partitioned into 512 point patches (sub-clouds), where each sub-cloud contains 32 points. To achieve this, we first perform the Farthest Point Sampling (FPS) operation to sample a representative skeleton and then employ the K-Nearest Neighbor (KNN) method to group neighboring points. For text descriptions and rendered images, we follow the pre-processing and augmentation procedures in CLIP [56, 8].

During pretraining, we freeze the text encoder, image encoder, and CLIP-ViT in the 3D encoder, updating only the parameters of modality-specific embeddings and the Perceiver.

3.2 Zero-Shot 3D Classification

3.2.1 Comparison with State-of-the-arts

Table 3: Zero-shot 3D classification on downstream datasets. Models are pretrained on ▶ULIP-ShapeNet Triplets, ▶ULIP2-Objaverse Triplets and ▶OpenShape Triplets. Measured in accuracy(%)

(a) Zero-shot 3D of classification on ModelNet40. Models are pretrained on ▶ULIP-ShapeNet Triplets.

Method	Training Source	Top1	Top5
ULIP-PointNet++(ssg)	▶	55.7	75.7
ULIP-PointNet++(msg)		58.4	78.2
ULIP-PointMLP		61.5	80.7
ULIP-PointBERT		60.4	84.0
VIT-LENS-OpenAI-B16		61.7	85.2
VIT-LENS-Laion2B-B16		65.4	92.7
VIT-LENS-OpenAI-L14		63.3	87.6
VIT-LENS-Datacomp-L14		70.6	94.4
		(+10.2)	(+10.4)

(b) Zero-shot 3D classification on ModelNet40. Models are pretrained on ▶ULIP2-Objaverse Triplets.

Method	Training Source	Top1	Top5
ULIP2-PointNeXt	▶	49.0	79.7
ULIP2-PointBERT		70.2	87.0
VIT-LENS-OpenAI-B16		73.4	92.0
VIT-LENS-Laion2B-B16		74.8	93.8
VIT-LENS-OpenAI-L14		76.1	93.2
VIT-LENS-Datacomp-L14		80.6	95.8
		(+10.4)	(+8.8)

(c) Zero-shot 3D classification on Objaverse-LVIS, ModelNet40 and ScanObjectNN. Models are pretrained on ▶OpenShape Triplets. “▶NO LVIS” denotes exclude all shapes from the Objaverse-LVIS subset. “▶All” means using all shapes from OpenShape Triplets.

Method	Training Source	Objaverse-LVIS			ModelNet40			ScanObjectNN		
		Top1	Top3	Top5	Top1	Top3	Top5	Top1	Top3	Top5
PointCLIP [75]	2D inferences, no 3D training	1.9	4.1	5.8	19.3	28.6	34.8	10.5	20.8	30.6
PointCLIP v2 [79]		4.7	9.5	12.9	63.6	77.9	85.0	42.1	63.3	74.5
ULIP-PointBERT [68]	▶NO LVIS	21.4	38.1	46.0	71.4	84.4	89.2	46.0	66.1	76.4
OpenShape-SparseConv [40]		37.0	58.4	66.9	82.6	95.0	97.5	54.9	76.8	87.0
OpenShape-PointBERT [40]		39.1	60.8	68.9	85.3	96.2	97.4	47.2	72.4	84.7
VIT-LENS-bigG14		50.1	71.3	78.1	86.8	96.8	97.8	59.8	79.3	87.7
		(+11.0)	(+10.5)	(+9.2)	(+1.5)	(+0.6)	(+0.3)	(+3.1)	(+2.5)	(+0.7)
ULIP-PointBERT [68]	▶All	26.8	44.8	52.6	75.1	88.1	93.2	51.6	72.5	82.3
OpenShape-SparseConv [40]		43.4	64.8	72.4	83.4	95.6	97.8	56.7	78.9	88.6
OpenShape-PointBERT [40]		46.8	69.1	77.0	84.4	96.5	98.0	52.2	79.7	88.7
VIT-LENS-bigG14		52.0	73.3	79.9	87.6	96.6	98.4	60.1	81.0	90.3
		(+5.2)	(+4.2)	(+2.9)	(+3.2)	(+0.1)	(+0.4)	(+3.4)	(+1.3)	(+1.6)

We conducted zero-shot classification evaluations of our models on three datasets: ModelNet40 [66], ScanObjectNN [61], and Objaverse-LVIS [11]. To ensure a fair comparison, we used the same datasets for pretraining as in previous works [68, 69, 40]. The comprehensive results can be found in Table 3.

In particular, we compared VIT-LENS with ULIP [68], using PointNet++ [54], PointMLP [43], and PointBERT [72] as 3D encoders. Table 3a presents the outcomes when our model is pretrained on ▶ULIP-Triplets. Notably, various variants of CLIP models employed in VIT-LENS outperform ULIP with different backbones. Particularly, using CLIP-ViT-L14 (Datacomp) [8] achieves a top-1 accuracy of 70.7% and a top-5 accuracy of 92.8% on ModelNet40, even surpassing ULIP2-PointBERT pretrained on the larger ▶ULIP2-Objaverse-Triplets.

The results of pretraining on ▶ULIP2-Triplets are presented in Table 3b. VIT-LENS with different variants significantly improves the zero-shot classification accuracy compared to ULIP2-PointNeXt [55] and ULIP2-PointBERT [72]. Notably, VIT-LENS with CLIP-ViT-L14 (Datacomp) [8] outperforms ULIP2-PointBERT by 10.4% in top-1 accuracy.

In Table 3c, we present the results of pretraining on the large-scale and text-enriched ▶OpenShape-Triplets. To align with OpenShape [40] and the released data, we adopted CLIP-ViT-bigG14 from Open CLIP [8] for VIT-LENS and trained on both ▶NO LVIS (excluding all shapes from the Objaverse-LVIS subset) and ▶All for comparison. VIT-LENS outperforms models adopted in OpenShape, even when their backbones are scaled for improved performance. Notably, VIT-LENS significantly improves the classification accuracy on the long-tail categories of Objaverse-LVIS, from 46.8% to 52.0%. Additionally, when pretrained on the NO LVIS subset, VIT-LENS achieves a top-1 accuracy of 50.2%. This outperformance is evident as it surpasses ULIP by approximately 30%, and even surpasses OpenShape-PointBERT, trained on the entire set, by 3.3%. These results demonstrate VIT-LENS’s capability to recognize open-world objects effectively. Regarding ModelNet40, VIT-LENS achieves an 87.4% accuracy, surpassing previous SOTAs on zero-shot classification and outperforming the fully-supervised 3D ShapeNets [66] and VoxNet [44]. Additionally, on ScanObjectNN, containing challenging real scans with noise and occlusion, our method exhibits decent sim-to-real transfer capabilities. VIT-LENS achieves a 60.6% zero-shot accuracy on ScanObjectNN without specific sim-to-real training, surpassing the previous SOTA.

3.2.2 Ablation Study

We perform various ablations by pretraining on ▶ULIP-ShapeNet Triplets [68] and evaluating on the ModelNet40 [66] zero-shot classification benchmarks, unless otherwise specified. The comprehensive results are presented in Table 4 and the default setting is marked with color , if applicable.

Comparison with PointBERT. We conduct experiments to compare VIT-LENS with PointBERT [72], a transformer based architecture for 3D point cloud understanding. This comparison involves aligning to the feature space of different CLIP variants and employing distinct pretraining datasets (refer to Table 1 and Table 2). As is shown in Table 4a, VIT-LENS outperforms PointBERT over all combinations of pretraining datasets and CLIP model for alignment. VIT-LENS consistently outperforms PointBERT across all conceivable combinations of pretraining datasets and CLIP models for alignment. This substantiates the efficacy of harnessing a pretrained ViT to advance 3D shape understanding.

Scaling pretraining dataset and model size. We investigate the effects of model size and pretraining data scale. Specifically, we choose OpenAI-B16 and OpenAI-L14 [56], both pretrained on WIT-400M, to ablate the model size. We conduct training on ▶ULIP-ShapeNet Triplets and ▶ULIP2-Objaverse Triplets to analyze the effect of dataset scale. The results in Figure 3 reveal that while keeping the dataset size constant, elevating the model scale from B16 to L14 enhances zero-shot performance, particularly noticeable for the larger L14 model. Moreover, when the model size is fixed, expanding the pretraining dataset yields improvements in model performance.

Comparing Scaling Capabilities of PointBERT and VIT-LENS. We evaluate the scalability of PointBERT [72] and VIT-LENS. Our experiments, depicted in Figure 4, involve varying both model sizes and pretraining datasets along the x-axis, ranging from ▶::Laion2B-B16 and ▶::Datacomp-L14 to ▶::bigG14. Here, the data scaling encompasses increases in dataset size and data quality. When scaling the model size

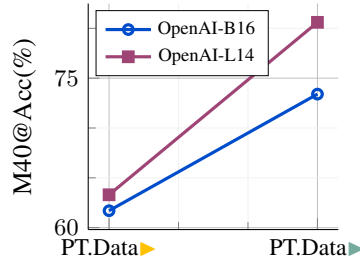


Figure 3: Zero-shot Classification Performance on ModelNet40. We assess the impact of model scaling using OpenAI-B16 and OpenAI-L14, and analyze the influence of pretraining datasets using ▶ and ▶.

Table 4: Ablation Study. We report top-1 zero-shot accuracy(%) on ModelNet40.

(a) More comparisons with PointBERT.			(b) Configuration of Perceiver on depth and parameters sharing.				(c) Effect of Perceiver #latents and ViT position embedding.			
PT.D.:CLIP Model	PointBERT	VIT-LENS	Depth	Share Weights	#T.param	Acc@1	#latents	ViT.pos	Flops	Acc@1
▶:: OpenAI-B16	60.2	61.7	2	-	34.1M	64.8	128	✗	54.0G	65.1
▶:: Laion2B-B16	62.6	65.4	4	✗	67.5M	64.2	128	✓	54.0G	65.2
▶:: OpenAI-L14	61.2	63.3	6	✗	100.8M	65.1	196	✗	75.4G	65.1
▶:: Datacomp-L14	65.4	70.6	4	✗	67.5M	64.2	196	✓	75.4G	65.4
▶:: OpenAI-B16	70.6	73.4	4	✓	34.1M	65.4	256	✗	94.6G	65.5
▶:: Laion2B-B16	71.7	74.8	6	✗	100.8M	65.1	256	✓	94.6G	65.5
▶:: OpenAI-L14	74.1	76.1	6	✓	34.1M	64.0	384	✗	136.4G	66.2
▶:: Datacomp-L14	77.8	80.6	8	✗	134.2M	64.0	384	✓	136.4G	66.3
▶:: bigG14	84.4	87.4	8	✓	34.1M	64.3	512	✗	179.5G	66.3
							512	✓	179.5G	67.4

(d) "Point Embedding→Perceiver" Performance.						(e) "Point Embedding→pretrained-ViT" Performance.				
Depth	#latents	Share Weights	#T.param	Flops	Acc@1	Unlocked Components in ViT		#T.param	Flops	Acc@1
2	196	-	34.1M	27.4G	62.2	None		7.3K	111.4G	50.0
4	196	✗	67.5M	40.5G	62.4	[CLS]		7.3K	111.4G	53.6
8	196	✗	134.6M	66.7G	62.7	[CLS], Proj		1.1M	111.4G	60.8
6	196	✗	101.2M	53.6G	61.9	[CLS], Proj, Block.1, Block.2		15.3M	111.4G	64.8
6	196	✓	34.1M	53.6G	62.3	[CLS], Proj, Block.11, Block.12		15.3M	111.4G	64.2
6	256	✗	101.3M	65.6G	63.5	[CLS], Proj, Block.1 - Block.4		29.5M	111.4G	65.4
6	256	✓	34.2M	65.6G	62.7	[CLS], Proj, Block.9 - Block.12		29.5M	111.4G	64.7
6	512	✗	101.5M	116.6G	62.5	[CLS], Proj, Block.1 - Block.6		43.7M	111.4G	66.4
6	512	✓	34.4M	116.6G	62.3	[CLS], Proj, Block.7 - Block.12		43.7M	111.4G	65.6
						All		86.6M	111.4G	67.7

Default Settings in VIT-LENS						Default Settings in VIT-LENS				
4	196	✓	34.1M	75.4G	65.4	None(tune PointEmb, Perceiver)		34.1M	75.4G	65.4

of VIT-LENS, we correspondingly scale up the PointBERT model. The results shown in Figure 4 underscore that VIT-LENS consistently outperforms PointBERT across all scaling configurations, owing to the rich knowledge encoded in the pretrained-ViT. Notably, when PointBERT is scaled to a large size (with 171M parameters), it achieves a top-1 zero-shot accuracy of 80.2%, lower than the use of a smaller PointBERT (with 32M parameters) for representation learning (*i.e.*, 84.4% zero-shot accuracy), similar to the findings in [40]. This substantiates that VIT-LENS excels in scalability.

Configuration of Perceiver in VIT-LENS. We study the effect of different design choices concerning the Perceiver [29] employed in VIT-LENS. Our study encompasses the ablation of Perceiver depth, representing the number of Perceiver blocks, as well as the exploration of parameter sharing beyond the second block (included). Results in Table 4b show that increasing the depth of Perceiver does not yield enhanced performance. Additionally, sharing parameters among Perceiver blocks proves capable of reducing parameters while achieving comparable or superior performance. This underscores the effectiveness and efficiency of the Perceiver architecture within VIT-LENS for connecting the 3D input to a pretrained-ViT.

Other hyper-parameters in VIT-LENS. We vary the number of latents used in the Perceiver architecture, which aligns with the sequence length of the pretrained-ViT input. As illustrated in Table 4c, employing a larger number of latents, such as 384 and 512, leads to slightly improved performance while concurrently increasing the GFlops. In this regard, we are able to harness the intrinsic capability of the Perceiver to extract insights from inputs of variable sizes and seamlessly connect them to the pretrained-ViT, thereby mitigating computational complexity. Furthermore, we investigate whether the inclusion of the pretrained-ViT position embedding influences model performance. In particular, we examine the case of CLIP Laion2B-B16 by interpolating the original position embedding while

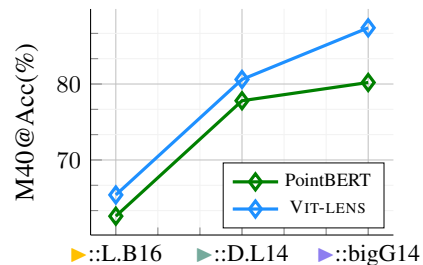


Figure 4: Scaling model size and pre-training data: PointBERT vs. VIT-LENS. In experiments, we compare PointBERT and the VIT-LENS’s encoder using identical pretraining dataset and CLIP model for alignment. VIT-LENS exhibits superior zero-shot performance and scalability.

varying the number of latents. The outcomes presented in Table 4c indicate that omitting the pretrained position embedding does not significantly degrade performance. We conjecture that the Perceiver has the capacity to implicitly assimilate position information on its own.

Point Embedding → Perceiver. To validate the efficacy of the pretrained-ViT, we investigate the performance of the “Point Embedding → Perceiver” paradigm. In this setup, the mean pooling feature of the Perceiver is directly aligned with the CLIP feature space. We execute experiments with various hyperparameter configurations, and the comprehensive outcomes are presented in Table 4d. Typically, the configuration employing a depth of 6 without parameter sharing possesses a comparable total parameter count to the default setting of VIT-LENS (~119M). Despite having less trainable parameters, VIT-LENS outperforms this variant by a significant margin. This observation underscores the pivotal role of harnessing the capabilities of the pretrained-ViT.

Point Embedding → pretrained-ViT. We also delve into the paradigm of “Point Embedding → pretrained-ViT”. As depicted in Table 4e, only training the Point Embedding yields a zero-shot accuracy of 50%, significantly lower than that of VIT-LENS due to the restricted number of trainable parameters. Furthermore, unlocking the transformer blocks for training leads to improved zero-shot performance. However, this tailored training approach optimized for 3D understanding might limit the adaptability of the resultant ViT to other modalities, thereby diminishing the pretrained-ViT’s overall generalization ability. Contrastingly, VIT-LENS attains commendable performance while largely retaining the core parameters of the pretrained-ViT, effectively harnessing its expansive knowledge across a wide array of modalities, with only a marginal increase in new parameters.

3.3 Emergent Capability: Connecting VIT-LENS to LLM Without Training

In this section, we study whether VIT-LENS’s representation can be used to unleash an LLM to understand the out-of-image modalities. Specifically, in this work, we use the 3D data for pilot experiment.

Preliminary for MLLM. Recent advancements in large language models (LLMs) have demonstrated remarkable emergent abilities, yet they lack the capacity to comprehend other modalities beyond text. Recent representation models have shown their bedrock role to unleash LLMs to understand, perceive, and interact with other modalities. For instance, Multimodal Large Language Models (MLLMs) effectively combine the LLMs and vision models, enabling reasoning with both textual and visual data. MLLMs not only provide human-like perception but also facilitate user-friendly interactions and a broader scope for solving diverse tasks.

Experimental Details of Unimodal Inputs. We use InstructBLIP [10], which is a versatile framework that enhances general-purpose models for a wide range of visual language tasks using a unified natural language interface by employing diverse instruction data to train an MLLM. InstructBLIP applies the pretrained EVA01-g14 [17] CLIP-ViT to perceive and encode images. Adhering to InstructBLIP’s configuration, we employ the EVA01-g14 CLIP for both images and texts, utilizing its CLIP-ViT as an integral part of the 3D encoder for point cloud encoding. We fine-tune the parameters of the point embedding and Perceiver on ►ULIP2-Objaverse Triplets. Following training, we seamlessly integrate VIT-LENS into InstructBLIP, enabling the resulting MLLM to effectively handle 3D input.

Our comparative analysis encompasses: (1) PointBERT aligned with the same CLIP model, replacing the post-training vision encoder in InstructBLIP; and (2) CLIPCap [47] from OpenShape [40]. We offer a snapshot of qualitative outcomes across different models in Table 5, Table 6, and Table 7. These examples spotlight several capabilities exhibited without specific MLLM tuning using 3D-related instruction data. Notably, the examples demonstrate that VIT-LENS empowers InstructBLIP to accurately describe 3D objects. For instance, the plant example in Table 5 is characterized as “sitting in a ceramic pot” and “bamboo-like”. Moreover, VIT-LENS excels in capturing nuanced visual concepts beyond the most prominent ones. For instance, the piano example reveals the observation of a “chair”.

For InstructBLIP w/ PointBERT, although PointBERT is able to conduct zero-shot classification, it fails to provide accurate information for the LLM to digest in such a zero-shot manner, and thus, InstructBLIP w/ PointBERT can not describe the 3D object correctly. CLIPCap-OpenShape, while displaying some relevant entities in captions (“vase” in Table 5 and “toilet” in Table 7), often leads to hallucinations and inaccurate captions.

Table 5: Example for VIT-LENS enabling MLLM to understand 3D inputs.

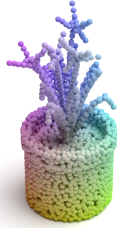
Visual input example, Plant:	
	
User	What is this object?
InstructBLIP w/ VIT-LENS	Potted plant.
User	Describe it in detail.
InstructBLIP w/ VIT-LENS	In the image, there is a potted plant sitting in a ceramic pot on a table. The plant appears to be a bamboo-like species, and it is positioned in such a way that its leaves appear to be growing out of the top of the pot. The plant's placement on the table suggests that it is meant to be a decorative element, adding a touch of greenery to the space. The ceramic pot has a diameter of around 10 centimeters, making it a suitable size for holding a small plant like this one. Overall, the image showcases a simple yet elegant arrangement of a potted plant in a ceramic pot on a table.
User	What is this object?
InstructBLIP w/ PointBERT	1000px by 1000px
User	Describe this object briefly.
InstructBLIP w/ PointBERT	A man in a suit and tie is standing in front of a desk.
CLIPCap-Openshape [47, 40]	Flowers in a vase, black and white.

Table 6: Example for VIT-LENS enabling MLLM to understand 3D inputs.

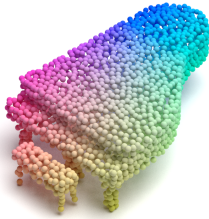
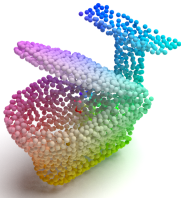
Visual input example, Piano:	
	
User	What is this object?
InstructBLIP w/ VIT-LENS	Piano.
User	What is the function of this?
InstructBLIP w/ VIT-LENS	Pianos are used to play music.
User	Describe it in detail.
InstructBLIP w/ VIT-LENS	The object in the image is an upright piano, which is a type of keyboard instrument known for its distinct sound and versatility. The piano is placed on a wooden surface, possibly a floor or a stage, and it appears to be quite large in size . Additionally, there is a chair placed next to the piano, suggesting that it may be used for seating during performances or lessons. The piano is positioned in the center of the image, making it the focal point of the scene. Overall, the combination of the piano and the chair creates an inviting atmosphere for music enthusiasts or those interested in learning how to play the piano.
User	What is this object?
InstructBLIP w/ PointBERT	Desk.
User	Describe this object briefly.
InstructBLIP w/ PointBERT	A black and white image of an office desk
CLIPCap-Openshape [47, 40]	A white house with a microphone in the middle of a dark room.

Table 7: Example for ViT-LENS enabling MLLM to understand 3D inputs.

Visual input example, Toilet:	
	
User	What is in the scene?
InstructBLIP w/ ViT-LENS	Toilet.
User	Describe it in detail.
InstructBLIP w/ ViT-LENS	The image features a close-up view of a toilet with its lid open, revealing the inside of the toilet bowl. The toilet appears to be made of porcelain or ceramic material, and it has a seat attached to it. The toilet is positioned on a white background, providing a clear and detailed view of the toilet’s design and construction. In addition to the toilet, there is another object in the image, which could be a piece of furniture or a decorative item, but it is not as prominent as the toilet. Overall, the image showcases a functional and well-designed toilet, emphasizing the importance of cleanliness and hygiene in daily life.
User	What is in the scene?
InstructBLIP w/ PointBERT	Lamp.
User	Describe this object briefly.
InstructBLIP w/ PointBERT	An image of a desk with a lamp on it.
CLIPCap-Openshape [47, 40]	The moment a man’s hand reaches out to touch a toilet bowl.

The overall results demonstrate that ViT-LENS excels not only at classifying the salient object of the 3D input, but also capturing the visual details, potentially attributed to the robustness of the pretrained-ViT, bringing the emergent ability to integrate with off-the-shelf LLM in a zero-shot manner.

Experimental Details for Multimodal Inputs. Following the previous setting, we plug the ViT-LENS into the InstructBLIP. Here, we show that a pretrained-ViT equipped with a variety of “lens” is a multimodal sensor that can perceive and integrate multimodalities simultaneously. To achieve this, we concatenate outputs from diverse modal lenses before the ViT transformer. The pretrained-ViT then encodes these concatenated embeddings and transmits the result to InstructBLIP for conditioned text generation. Our specific experiment involves the fusion of image[†] and point cloud data.

Qualitative outcomes are presented in Table 8 for dual multimodal inputs (a point cloud instance and an image) and in Table 9 for tri-modal inputs (a point cloud instance and 2 images). The responses from InstructBLIP w/ ViT-LENS underscore its adaptability in seamlessly integrating diverse modalities, allowing InstructBLIP to interpret multimodal inputs as it is viewing an image. Notably, this integration empowers the resulting MLLM to depict multimodal inputs, discern unconventional co-occurrence of concepts from different modalities, and craft narratives based on the integrated information of multimodalities.

[†]Photos credited to <https://www.pexels.com/>.

Table 8: Example to illustrate the Instruct-BLIP with two multimodal inputs.

InstructBLIP w/ ViT-LENS, Two Multimodal Inputs.

Example 1: 3D Point Cloud + Image



Prompt 1: Describe based on what you see.

Response 1: An image of a piano with the earth in the background.

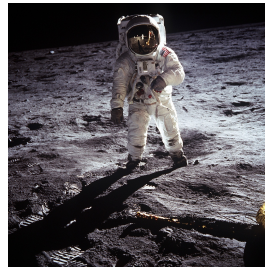
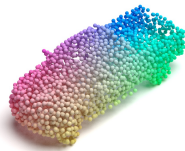
Prompt 2: What is unusual about this image?

Response 2: The unusual aspect of this image is that it depicts a piano floating in space, with the Earth visible in the background. This is an imaginative and creative representation of a musical instrument in an unconventional setting, showcasing its versatility and adaptability to different environments.

Prompt 3: Imagine the events leading up to this moment and those that follow. Create a story that links them together.

Response 3: In the image, we see a grand piano placed on top of the earth, with the moon and stars visible in the background. This setting creates a unique and captivating scene that invites the viewer to imagine the events leading up to this moment and those that follow. One possible storyline could involve a talented pianist who has always dreamed of performing on top of the earth. After years of hard work and dedication, they finally have the opportunity to make their dream come true. As they prepare for their performance, they reflect on the journey that led them to this moment and the challenges they faced along the way. During their performance, they play a beautiful melody that captures the essence of the earth's beauty and the vastness of the universe. The audience is mesmerized by the performance, and the pianist feels a sense of accomplishment and fulfillment as they conclude their performance on top of the earth.

Example 2: 3D Point Cloud + Image



Prompt 1: Imagine you are a narrator looking at this, describe the essence of what you see.

Response 1: An astronaut standing next to a pickup truck on the surface of the moon.

Prompt 2: What is unusual about this image?

Response 2: The unusual aspect of this image is that it depicts an astronaut standing on the surface of the moon with a pickup truck in the foreground. This combination of elements is not commonly associated with space exploration or the moon's surface, making it an unconventional and eye-catching image.

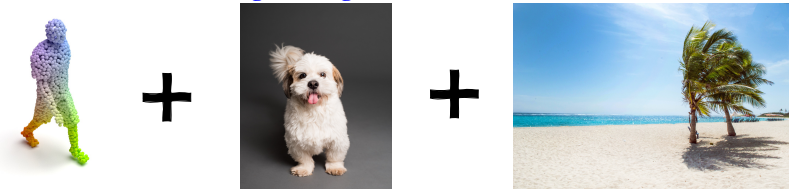
Prompt 3: Craft a narrative based on the visual elements in the picture. Let your imagination guide the story.

Response 3: In the image, an astronaut is standing on the moon's surface with a pickup truck in the background. The astronaut is wearing a spacesuit and appears to be exploring the lunar terrain. The pickup truck is parked on the moon's surface, adding a unique touch to the scene. The combination of the astronaut and the pickup truck creates an intriguing narrative that invites the viewer to imagine what might be happening in this futuristic setting.

Table 9: Example to illustrate the Instruct-BLIP with three multimodal inputs.

InstructBLIP w/ VIT-LENS, Three Multimodal Inputs.

Example 1: 3D Point Cloud + Image + Image



Prompt 1: Describe the scene based on what you see.

Response 1: A man walking a dog on a beach with palm trees in the background.

Prompt 2: Describe the details of what you see.

Response 2: The image depicts a man and his dog walking on a sandy beach. The man is holding the dog's leash, while the dog appears to be enjoying its time on the beach. In the background, there is a palm tree visible, adding to the serene atmosphere of the scene. The man and the dog seem to be in good spirits, enjoying each other's company as they stroll along the beach.

Prompt 3: Imagine the events leading up to this moment and those that follow. Create a story that links them together.

Response 3: In the story, the man and his dog are walking along the beach, enjoying the sunny day. As they walk, the man notices a piece of paper lying on the sand. Curious, he picks it up and discovers that it's an advertisement for a photography contest. The man decides to enter the contest and submits a photo of himself and his dog on the beach. To his surprise, his photo is selected as one of the winners, and he is invited to attend the award ceremony. At the event, he meets other photographers and learns more about the art of photography. Through this experience, the man gains a new appreciation for photography and decides to pursue it as a hobby. He continues to take photos of his dog and other subjects, honing his skills and capturing unique moments in time. Eventually, his passion for photography leads him to become a professional photographer, and he shares his work with others, inspiring them to appreciate the beauty of the world around them.

Example 2: 3D Point Cloud + Image + Image



Prompt 1: Describe what you see.

Response 1: A man walking down a road with the earth in the background.

Prompt 2: What is unusual about this image?

Response 2: The unusual aspect of this image is that it depicts a man walking on a road, but the background appears to be a space scene with a planet in the distance. This combination of elements creates a surreal and futuristic atmosphere, making the image stand out as unconventional and visually striking. The man's presence on the road and the planet in the background create a sense of contrast between the mundane and the extraordinary, adding an element of surprise and intrigue to the image.

Prompt 3: Craft a narrative based on the visual elements in the picture. Let your imagination guide the story.

Response 3: As you look at the image, you see a man standing on a road with a planet in the background. The man is wearing a shirt and shorts, and he appears to be contemplating something as he stands on the road. The planet in the background adds a sense of wonder and exploration to the scene, as if the man is pondering the vastness of the universe and his place within it. Perhaps he is reflecting on his journey so far, or perhaps he is planning his next adventure. In any case, the combination of the man, the road, and the planet creates an intriguing narrative that invites the viewer's imagination to fill in the details.

4 Related Work

Vision Language Pretraining. Training images together with linguistic signals, such as words or sentences, has proven to be a powerful approach for tasks like zero-shot recognition and text-to-image retrieval [14, 18, 32, 59]. Leveraging language as supervision has also been beneficial for learning robust video representations [2, 45, 46]. In [31], large-scale image datasets with noisy captions were shown to yield strong visual features. Recent advancements in vision-language pretraining, such as CLIP [56], ALIGN [30], and Florence [73], have collected extensive image and text pairs and trained models to embed both modalities in a shared space using contrastive learning, leading to impressive zero-shot performance. CoCa [71] introduced an image captioning objective along with contrastive loss for further improvement. Flamingo [1] handles interleaved images and texts and achieves state-of-the-art results on various few-shot learning benchmarks. LiT [74] utilizes contrastive training for fine-tuning and observes that freezing image encoders yields the best results. While prior works primarily focus on image and text modalities, VIT-LENS aims to extend the capability of zero-shot recognition to multiple modalities, enabling comprehensive multimodal understanding.

Align to CLIP. Pretrained CLIP models have emerged as effective teachers to guide other models due to the robustness of their visual representations [53, 17, 65]. Beyond its role as a teacher, CLIP’s joint image and text embedding space has been harnessed for a diverse set of zero-shot tasks, such as segmentation [33], detection [25, 77], 3D shape understanding [68, 69, 40, 75, 79], 3D open-vocabulary segmentation [52], mesh animation [70], and more, showcasing the efficacy of this joint embedding space. In contrast to merely aligning with CLIP’s embedding space, VIT-LENS goes a step further by capitalizing on the capabilities of the powerful pretrained-ViT to comprehend and interpret diverse modalities, significantly enhancing its multi-modal understanding capabilities. By enabling a pretrained-ViT to extend beyond its original scope of images, VIT-LENS achieves comprehensive multimodal understanding, paving the way for enhanced zero-shot recognition across a wide range of modalities and tasks.

Advances in Multimodal Learning. Previous research has explored various approaches for jointly training multiple modalities, either in supervised [24, 36, 20] or self-supervised settings [23, 3, 60, 48, 37]. The effectiveness of image and language pretraining methods, exemplified by CLIP, has sparked investigations into leveraging such approaches to learn deep semantic representations by aligning other modalities with textual inputs. Several methods have adapted CLIP to extract semantically rich representations from different modalities [42, 38, 15, 67, 21]. In the context of multimodal zero-shot learning, several approaches have been proposed to align various modalities to CLIP. For instance, AudioCLIP [27] incorporates audio as an additional modality into the CLIP framework, enabling zero-shot audio classification. ImageBind [22] aligns six modalities to CLIP using paired image data. ONE-PEACE [63] introduces a unified encoder that is pretrained from scratch to align vision, language, and audio. Zhang *et al.* [76] pretrain a transformer with LAION-2B following the CLIP methodology and freeze the resulting transformer for downstream tasks involving different modalities. In contrast, VIT-LENS takes a unique approach by empowering a pretrained-ViT to effectively comprehend and bind diverse modalities without the need for any manual annotations.

5 Conclusion

In this paper, we present VIT-LENS, a novel approach for advancing omni-modal representation learning by leveraging a pretrained-ViT to comprehend diverse modalities. Our method views a pretrained-ViT as a multi-modal sensor capable of perceiving various modalities, eliminating the need for separate architectures for different modalities and reducing the burden of large-scale data collection. In our evaluation of VIT-LENS in 3D shape understanding, we found that VIT-LENS representations effectively capture a wide range of semantic and visual concepts, enabling superior capabilities for open-world 3D shape recognition. By binding 3D shapes to ViT, our model can be integrated with off-the-shelf MLLM, showcasing its potential to enable LLMs to understand and interact with 3D data in a zero-shot manner. VIT-LENS aims to pave the way towards comprehensive omni-modal representation learning without requiring large-scale data collection, presenting a scalable and efficient solution for leveraging the power of pretrained models in diverse applications. Future work can explore further extensions to additional modalities and emergent abilities to drive advancements in the field of omni-modal representation learning.

References

- [1] Jean-Baptiste Alayrac, Jeff Donahue, Pauline Luc, Antoine Miech, Iain Barr, Yana Hasson, Karel Lenc, Arthur Mensch, Katie Millican, Malcolm Reynolds, et al. Flamingo: a visual language model for few-shot learning. *arXiv preprint arXiv:2204.14198*, 2022.
- [2] Jean-Baptiste Alayrac, Adria Recasens, Rosalia Schneider, Relja Arandjelović, Jason Ramapuram, Jeffrey De Fauw, Lucas Smaira, Sander Dieleman, and Andrew Zisserman. Self-supervised multimodal versatile networks. *Advances in Neural Information Processing Systems*, 33:25–37, 2020.
- [3] Relja Arandjelovic and Andrew Zisserman. Look, listen and learn. In *Proceedings of the IEEE international conference on computer vision*, pages 609–617, 2017.
- [4] Hangbo Bao, Li Dong, and Furu Wei. Beit: Bert pre-training of image transformers. *arXiv preprint arXiv:2106.08254*, 2021.
- [5] Tom Brown, Benjamin Mann, Nick Ryder, Melanie Subbiah, Jared D Kaplan, Prafulla Dhariwal, Arvind Neelakantan, Pranav Shyam, Girish Sastry, Amanda Askell, et al. Language models are few-shot learners. *NeurIPS*, pages 1877–1901, 2020.
- [6] Mathilde Caron, Hugo Touvron, Ishan Misra, Hervé Jégou, Julien Mairal, Piotr Bojanowski, and Armand Joulin. Emerging properties in self-supervised vision transformers. In *Proceedings of the IEEE/CVF international conference on computer vision*, pages 9650–9660, 2021.
- [7] Angel X Chang, Thomas Funkhouser, Leonidas Guibas, Pat Hanrahan, Qixing Huang, Zimo Li, Silvio Savarese, Manolis Savva, Shuran Song, Hao Su, et al. Shapenet: An information-rich 3d model repository. *arXiv preprint arXiv:1512.03012*, 2015.
- [8] Mehdi Cherti, Romain Beaumont, Ross Wightman, Mitchell Wortsman, Gabriel Ilharco, Cade Gordon, Christoph Schuhmann, Ludwig Schmidt, and Jenia Jitsev. Reproducible scaling laws for contrastive language-image learning. *arXiv preprint arXiv:2212.07143*, 2022.
- [9] Jasmine Collins, Shubham Goel, Kenan Deng, Achleshwar Luthra, Leon Xu, Erhan Gundogdu, Xi Zhang, Tomas F Yago Vicente, Thomas Dideriksen, Himanshu Arora, et al. Abo: Dataset and benchmarks for real-world 3d object understanding. In *Proceedings of the IEEE/CVF Conference on Computer Vision and Pattern Recognition*, pages 21126–21136, 2022.
- [10] Wenliang Dai, Junnan Li, Dongxu Li, Anthony Meng Huat Tiong, Junqi Zhao, Weisheng Wang, Boyang Li, Pascale Fung, and Steven Hoi. Instructblip: Towards general-purpose vision-language models with instruction tuning. *arXiv preprint arXiv:2305.06500*, 2023.
- [11] Matt Deitke, Dustin Schwenk, Jordi Salvador, Luca Weihs, Oscar Michel, Eli VanderBilt, Ludwig Schmidt, Kiana Ehsani, Aniruddha Kembhavi, and Ali Farhadi. Objaverse: A universe of annotated 3d objects. In *Proceedings of the IEEE/CVF Conference on Computer Vision and Pattern Recognition*, pages 13142–13153, 2023.
- [12] Jacob Devlin, Ming-Wei Chang, Kenton Lee, and Kristina Toutanova. Bert: Pre-training of deep bidirectional transformers for language understanding. *arXiv preprint arXiv:1810.04805*, 2018.
- [13] Alexey Dosovitskiy, Lucas Beyer, Alexander Kolesnikov, Dirk Weissenborn, Xiaohua Zhai, Thomas Unterthiner, Mostafa Dehghani, Matthias Minderer, Georg Heigold, Sylvain Gelly, et al. An image is worth 16x16 words: Transformers for image recognition at scale. *arXiv preprint arXiv:2010.11929*, 2020.
- [14] Fartash Faghri, David J Fleet, Jamie Ryan Kiros, and Sanja Fidler. Vse++: Improving visual-semantic embeddings with hard negatives. *arXiv preprint arXiv:1707.05612*, 2017.
- [15] Han Fang, Pengfei Xiong, Luhui Xu, and Yu Chen. Clip2video: Mastering video-text retrieval via image clip. *arXiv preprint arXiv:2106.11097*, 2021.
- [16] Yuxin Fang, Quan Sun, Xinggang Wang, Tiejun Huang, Xinlong Wang, and Yue Cao. Eva-02: A visual representation for neon genesis. *arXiv preprint arXiv:2303.11331*, 2023.

- [17] Yuxin Fang, Wen Wang, Binhui Xie, Quan Sun, Ledell Wu, Xinggang Wang, Tiejun Huang, Xinlong Wang, and Yue Cao. Eva: Exploring the limits of masked visual representation learning at scale. In *Proceedings of the IEEE/CVF Conference on Computer Vision and Pattern Recognition*, pages 19358–19369, 2023.
- [18] Andrea Frome, Greg S Corrado, Jon Shlens, Samy Bengio, Jeff Dean, Marc’Aurelio Ranzato, and Tomas Mikolov. Devise: A deep visual-semantic embedding model. *Advances in neural information processing systems*, 26, 2013.
- [19] Huan Fu, Rongfei Jia, Lin Gao, Mingming Gong, Binqiang Zhao, Steve Maybank, and Dacheng Tao. 3d-future: 3d furniture shape with texture. *International Journal of Computer Vision*, 129:3313–3337, 2021.
- [20] Difei Gao, Ke Li, Ruiping Wang, Shiguang Shan, and Xilin Chen. Multi-modal graph neural network for joint reasoning on vision and scene text. In *Proceedings of the IEEE/CVF conference on computer vision and pattern recognition*, pages 12746–12756, 2020.
- [21] Difei Gao, Luowei Zhou, Lei Ji, Linchao Zhu, Yi Yang, and Mike Zheng Shou. Mist: Multi-modal iterative spatial-temporal transformer for long-form video question answering. In *Proceedings of the IEEE/CVF Conference on Computer Vision and Pattern Recognition*, pages 14773–14783, 2023.
- [22] Rohit Girdhar, Alaaeldin El-Nouby, Zhuang Liu, Mannat Singh, Kalyan Vasudev Alwala, Armand Joulin, and Ishan Misra. Imagebind: One embedding space to bind them all. In *Proceedings of the IEEE/CVF Conference on Computer Vision and Pattern Recognition*, pages 15180–15190, 2023.
- [23] Rohit Girdhar, Alaaeldin El-Nouby, Mannat Singh, Kalyan Vasudev Alwala, Armand Joulin, and Ishan Misra. Omnima: Single model masked pretraining on images and videos. In *Proceedings of the IEEE/CVF Conference on Computer Vision and Pattern Recognition*, pages 10406–10417, 2023.
- [24] Rohit Girdhar, Mannat Singh, Nikhila Ravi, Laurens van der Maaten, Armand Joulin, and Ishan Misra. Omnivore: A single model for many visual modalities. In *Proceedings of the IEEE/CVF Conference on Computer Vision and Pattern Recognition*, pages 16102–16112, 2022.
- [25] Xiuye Gu, Tsung-Yi Lin, Weicheng Kuo, and Yin Cui. Open-vocabulary object detection via vision and language knowledge distillation. *arXiv preprint arXiv:2104.13921*, 2021.
- [26] Agrim Gupta, Piotr Dollar, and Ross Girshick. Lvis: A dataset for large vocabulary instance segmentation. In *Proceedings of the IEEE/CVF conference on computer vision and pattern recognition*, pages 5356–5364, 2019.
- [27] Andrey Guzhov, Federico Raue, Jörn Hees, and Andreas Dengel. Audioclip: Extending clip to image, text and audio. In *ICASSP 2022-2022 IEEE International Conference on Acoustics, Speech and Signal Processing (ICASSP)*, pages 976–980. IEEE, 2022.
- [28] Kaiming He, Xinlei Chen, Saining Xie, Yanghao Li, Piotr Dollár, and Ross Girshick. Masked autoencoders are scalable vision learners. In *Proceedings of the IEEE/CVF conference on computer vision and pattern recognition*, pages 16000–16009, 2022.
- [29] Andrew Jaegle, Felix Gimeno, Andy Brock, Oriol Vinyals, Andrew Zisserman, and Joao Carreira. Perceiver: General perception with iterative attention. In *International conference on machine learning*, pages 4651–4664. PMLR, 2021.
- [30] Chao Jia, Yinfei Yang, Ye Xia, Yi-Ting Chen, Zarana Parekh, Hieu Pham, Quoc Le, Yun-Hsuan Sung, Zhen Li, and Tom Duerig. Scaling up visual and vision-language representation learning with noisy text supervision. In *International conference on machine learning*, pages 4904–4916. PMLR, 2021.
- [31] Armand Joulin, Laurens Van Der Maaten, Allan Jabri, and Nicolas Vasilache. Learning visual features from large weakly supervised data. In *Computer Vision—ECCV 2016: 14th European Conference, Amsterdam, The Netherlands, October 11–14, 2016, Proceedings, Part VII 14*, pages 67–84. Springer, 2016.

- [32] Ryan Kiros, Ruslan Salakhutdinov, and Richard S Zemel. Unifying visual-semantic embeddings with multimodal neural language models. *arXiv preprint arXiv:1411.2539*, 2014.
- [33] Boyi Li, Kilian Q Weinberger, Serge Belongie, Vladlen Koltun, and Rene Ranftl. Language-driven semantic segmentation. In *International Conference on Learning Representations*, 2022.
- [34] Junnan Li, Dongxu Li, Silvio Savarese, and Steven Hoi. Blip-2: Bootstrapping language-image pre-training with frozen image encoders and large language models. *arXiv preprint arXiv:2301.12597*, 2023.
- [35] Junnan Li, Dongxu Li, Caiming Xiong, and Steven Hoi. Blip: Bootstrapping language-image pre-training for unified vision-language understanding and generation. In *ICML*, pages 12888–12900, 2022.
- [36] Valerii Likhoshesterov, Anurag Arnab, Krzysztof Choromanski, Mario Lucic, Yi Tay, Adrian Weller, and Mostafa Dehghani. Polyvit: Co-training vision transformers on images, videos and audio. *arXiv preprint arXiv:2111.12993*, 2021.
- [37] Kevin Qinghong Lin, Jinpeng Wang, Mattia Soldan, Michael Wray, Rui Yan, Eric Z XU, Difei Gao, Rong-Cheng Tu, Wenzhe Zhao, Weijie Kong, et al. Egocentric video-language pretraining. *Advances in Neural Information Processing Systems*, 35:7575–7586, 2022.
- [38] Ziyi Lin, Shijie Geng, Renrui Zhang, Peng Gao, Gerard de Melo, Xiaogang Wang, Jifeng Dai, Yu Qiao, and Hongsheng Li. Frozen clip models are efficient video learners. In *European Conference on Computer Vision*, pages 388–404. Springer, 2022.
- [39] Haotian Liu, Chunyuan Li, Qingyang Wu, and Yong Jae Lee. Visual instruction tuning. *arXiv preprint arXiv:2304.08485*, 2023.
- [40] Minghua Liu, Ruoxi Shi, Kaiming Kuang, Yin hao Zhu, Xuanlin Li, Shizhong Han, Hong Cai, Fatih Porikli, and Hao Su. Openshape: Scaling up 3d shape representation towards open-world understanding. *arXiv preprint arXiv:2305.10764*, 2023.
- [41] Yinhan Liu, Myle Ott, Naman Goyal, Jingfei Du, Mandar Joshi, Danqi Chen, Omer Levy, Mike Lewis, Luke Zettlemoyer, and Veselin Stoyanov. Roberta: A robustly optimized bert pretraining approach. *arXiv preprint arXiv:1907.11692*, 2019.
- [42] Huaishao Luo, Lei Ji, Ming Zhong, Yang Chen, Wen Lei, Nan Duan, and Tianrui Li. Clip4clip: An empirical study of clip for end to end video clip retrieval and captioning. *Neurocomputing*, 508:293–304, 2022.
- [43] Xu Ma, Can Qin, Haoxuan You, Haoxi Ran, and Yun Fu. Rethinking network design and local geometry in point cloud: A simple residual mlp framework. *arXiv preprint arXiv:2202.07123*, 2022.
- [44] Daniel Maturana and Sebastian Scherer. Voxnet: A 3d convolutional neural network for real-time object recognition. In *2015 IEEE/RSJ international conference on intelligent robots and systems (IROS)*, pages 922–928. IEEE, 2015.
- [45] Antoine Miech, Jean-Baptiste Alayrac, Lucas Smaira, Ivan Laptev, Josef Sivic, and Andrew Zisserman. End-to-end learning of visual representations from uncurated instructional videos. In *Proceedings of the IEEE/CVF Conference on Computer Vision and Pattern Recognition*, pages 9879–9889, 2020.
- [46] Antoine Miech, Dimitri Zhukov, Jean-Baptiste Alayrac, Makarand Tapaswi, Ivan Laptev, and Josef Sivic. Howto100m: Learning a text-video embedding by watching hundred million narrated video clips. In *Proceedings of the IEEE/CVF International Conference on Computer Vision*, pages 2630–2640, 2019.
- [47] Ron Mokady, Amir Hertz, and Amit H Bermano. Clipcap: Clip prefix for image captioning. *arXiv preprint arXiv:2111.09734*, 2021.

- [48] Pedro Morgado, Nuno Vasconcelos, and Ishan Misra. Audio-visual instance discrimination with cross-modal agreement. In *Proceedings of the IEEE/CVF Conference on Computer Vision and Pattern Recognition*, pages 12475–12486, 2021.
- [49] OpenAI. Introducing chatgpt. OpenAI Blog, 09 2021.
- [50] OpenAI. Gpt-4 technical report, 2023.
- [51] Maxime Oquab, Timothée Darcet, Théo Moutakanni, Huy Vo, Marc Szafraniec, Vasil Khalidov, Pierre Fernandez, Daniel Haziza, Francisco Massa, Alaaeldin El-Nouby, et al. Dinov2: Learning robust visual features without supervision. *arXiv preprint arXiv:2304.07193*, 2023.
- [52] Songyou Peng, Kyle Genova, Chiyu "Max" Jiang, Andrea Tagliasacchi, Marc Pollefeys, and Thomas Funkhouser. Openscene: 3d scene understanding with open vocabularies. In *Proceedings of the IEEE/CVF Conference on Computer Vision and Pattern Recognition*, 2023.
- [53] Zhiliang Peng, Li Dong, Hangbo Bao, Qixiang Ye, and Furu Wei. Beit v2: Masked image modeling with vector-quantized visual tokenizers. *arXiv preprint arXiv:2208.06366*, 2022.
- [54] Charles Ruizhongtai Qi, Li Yi, Hao Su, and Leonidas J Guibas. Pointnet++: Deep hierarchical feature learning on point sets in a metric space. *Advances in neural information processing systems*, 30, 2017.
- [55] Guocheng Qian, Yuchen Li, Houwen Peng, Jinjie Mai, Hasan Hammoud, Mohamed Elhoseiny, and Bernard Ghanem. Pointnext: Revisiting pointnet++ with improved training and scaling strategies. *Advances in Neural Information Processing Systems*, 35:23192–23204, 2022.
- [56] Alec Radford, Jong Wook Kim, Chris Hallacy, Aditya Ramesh, Gabriel Goh, Sandhini Agarwal, Girish Sastry, Amanda Askell, Pamela Mishkin, Jack Clark, et al. Learning transferable visual models from natural language supervision. In *International conference on machine learning*, pages 8748–8763. PMLR, 2021.
- [57] Alec Radford, Karthik Narasimhan, Tim Salimans, Ilya Sutskever, et al. Improving language understanding by generative pre-training. 2018.
- [58] Alec Radford, Jeffrey Wu, Rewon Child, David Luan, Dario Amodei, Ilya Sutskever, et al. Language models are unsupervised multitask learners. *OpenAI blog*, page 9, 2019.
- [59] Richard Socher, Andrej Karpathy, Quoc V Le, Christopher D Manning, and Andrew Y Ng. Grounded compositional semantics for finding and describing images with sentences. *Transactions of the Association for Computational Linguistics*, 2:207–218, 2014.
- [60] Yonglong Tian, Dilip Krishnan, and Phillip Isola. Contrastive multiview coding. In *Computer Vision—ECCV 2020: 16th European Conference, Glasgow, UK, August 23–28, 2020, Proceedings, Part XI 16*, pages 776–794. Springer, 2020.
- [61] Mikaela Angelina Uy, Quang-Hieu Pham, Binh-Son Hua, Thanh Nguyen, and Sai-Kit Yeung. Revisiting point cloud classification: A new benchmark dataset and classification model on real-world data. In *Proceedings of the IEEE/CVF international conference on computer vision*, pages 1588–1597, 2019.
- [62] Ashish Vaswani, Noam Shazeer, Niki Parmar, Jakob Uszkoreit, Llion Jones, Aidan N Gomez, Łukasz Kaiser, and Illia Polosukhin. Attention is all you need. *Advances in neural information processing systems*, 30, 2017.
- [63] Peng Wang, Shijie Wang, Junyang Lin, Shuai Bai, Xiaohuan Zhou, Jingren Zhou, Xinggang Wang, and Chang Zhou. One-peace: Exploring one general representation model toward unlimited modalities. *arXiv preprint arXiv:2305.11172*, 2023.
- [64] Wenhui Wang, Hangbo Bao, Li Dong, Johan Bjorck, Zhiliang Peng, Qiang Liu, Kriti Aggarwal, Owais Khan Mohammed, Saksham Singhal, Subhojit Som, and Furu Wei. Image as a foreign language: BEiT pretraining for vision and vision-language tasks. In *Proceedings of the IEEE/CVF Conference on Computer Vision and Pattern Recognition*, 2023.

- [65] Yixuan Wei, Han Hu, Zhenda Xie, Zheng Zhang, Yue Cao, Jianmin Bao, Dong Chen, and Baining Guo. Contrastive learning rivals masked image modeling in fine-tuning via feature distillation. *arXiv preprint arXiv:2205.14141*, 2022.
- [66] Zhirong Wu, Shuran Song, Aditya Khosla, Fisher Yu, Linguang Zhang, Xiaoou Tang, and Jianxiong Xiao. 3d shapenets: A deep representation for volumetric shapes. In *Proceedings of the IEEE conference on computer vision and pattern recognition*, pages 1912–1920, 2015.
- [67] Hongwei Xue, Yuchong Sun, Bei Liu, Jianlong Fu, Ruihua Song, Houqiang Li, and Jiebo Luo. Clip-vip: Adapting pre-trained image-text model to video-language representation alignment. *arXiv preprint arXiv:2209.06430*, 2022.
- [68] Le Xue, Mingfei Gao, Chen Xing, Roberto Martín-Martín, Jiajun Wu, Caiming Xiong, Ran Xu, Juan Carlos Niebles, and Silvio Savarese. Ulip: Learning a unified representation of language, images, and point clouds for 3d understanding. In *Proceedings of the IEEE/CVF Conference on Computer Vision and Pattern Recognition*, pages 1179–1189, 2023.
- [69] Le Xue, Ning Yu, Shu Zhang, Junnan Li, Roberto Martín-Martín, Jiajun Wu, Caiming Xiong, Ran Xu, Juan Carlos Niebles, and Silvio Savarese. Ulip-2: Towards scalable multimodal pre-training for 3d understanding. *arXiv preprint arXiv:2305.08275*, 2023.
- [70] Kim Youwang, Kim Ji-Yeon, and Tae-Hyun Oh. Clip-actor: Text-driven recommendation and stylization for animating human meshes. In *ECCV*, 2022.
- [71] Jiahui Yu, Zirui Wang, Vijay Vasudevan, Legg Yeung, Mojtaba Seyedhosseini, and Yonghui Wu. Coca: Contrastive captioners are image-text foundation models. *arXiv preprint arXiv:2205.01917*, 2022.
- [72] Xumin Yu, Lulu Tang, Yongming Rao, Tiejun Huang, Jie Zhou, and Jiwen Lu. Point-bert: Pre-training 3d point cloud transformers with masked point modeling. In *Proceedings of the IEEE/CVF Conference on Computer Vision and Pattern Recognition*, pages 19313–19322, 2022.
- [73] Lu Yuan, Dongdong Chen, Yi-Ling Chen, Noel Codella, Xiyang Dai, Jianfeng Gao, Houdong Hu, Xuedong Huang, Boxin Li, Chunyuan Li, et al. Florence: A new foundation model for computer vision. *arXiv preprint arXiv:2111.11432*, 2021.
- [74] Xiaohua Zhai, Xiao Wang, Basil Mustafa, Andreas Steiner, Daniel Keysers, Alexander Kolesnikov, and Lucas Beyer. Lit: Zero-shot transfer with locked-image text tuning. In *Proceedings of the IEEE/CVF Conference on Computer Vision and Pattern Recognition*, pages 18123–18133, 2022.
- [75] Renrui Zhang, Ziyu Guo, Wei Zhang, Kunchang Li, Xupeng Miao, Bin Cui, Yu Qiao, Peng Gao, and Hongsheng Li. Pointclip: Point cloud understanding by clip. In *Proceedings of the IEEE/CVF Conference on Computer Vision and Pattern Recognition*, pages 8552–8562, 2022.
- [76] Yiyuan Zhang, Kaixiong Gong, Kaipeng Zhang, Hongsheng Li, Yu Qiao, Wanli Ouyang, and Xiangyu Yue. Meta-transformer: A unified framework for multimodal learning. *arXiv preprint arXiv:2307.10802*, 2023.
- [77] Xingyi Zhou, Rohit Girdhar, Armand Joulin, Philipp Krähenbühl, and Ishan Misra. Detecting twenty-thousand classes using image-level supervision. In *European Conference on Computer Vision*, pages 350–368. Springer, 2022.
- [78] Deyao Zhu, Jun Chen, Xiaoqian Shen, Xiang Li, and Mohamed Elhoseiny. Minigtpt-4: Enhancing vision-language understanding with advanced large language models, 2023.
- [79] Xiangyang Zhu, Renrui Zhang, Bowei He, Ziyao Zeng, Shanghang Zhang, and Peng Gao. Point-clip v2: Adapting clip for powerful 3d open-world learning. *arXiv preprint arXiv:2211.11682*, 2022.